Available online at www.sciencedirect.com
ScienceDirect
Journal of Catalysis 247 (2007) 288–297
JOURNAL OF CATALYSIS
www.elsevier.com/locate/jcat

Plasma catalysis with perovskite-type catalysts for the removal of NO and CH_4 from combustion exhausts

J.L. Hueso [a,b], J. Cotrino [a,c], A. Caballero [a,b], J.P. Espinós [a,b], A.R. González-Elipe [a,b,*]

[a] *Instituto de Ciencia de Materiales de Sevilla (CSIC – University of Seville), Avda. Américo Vespucio, 49, 41092 Seville, Spain*
[b] *Departamento de Química Inorgánica, Universidad de Sevilla, Spain*
[c] *Departamento de Física Atómica, Molecular y Nuclear, Universidad de Sevilla, Spain*

Received 6 December 2006; revised 2 February 2007; accepted 2 February 2007

Available online 21 March 2007

Abstract

The removal of NO and CH_4 from quaternary gas mixtures simulating the conditions existing in real combustion exhausts has been studied with a hybrid system integrating plasma activation and a $La_{1-x}Sr_xCoO_{3-d}$ perovskite-type catalyst. The plasma reaction produces the conversion of NO into N_2 plus O_2 and the oxidation of CH_4 into CO + H_2O. Incorporation of the catalyst favors the oxidation of CH_4 into CO_2 at 190 °C. At this temperature, no oxidation of CO or CH_4 is found in a conventional catalytic reactor. A similar plasma + catalyst experiment with SiO_2 found much lower CO_2 production, indicating that the perovskite is actively involved in the oxidation of CO. The efficiency of NO removal decreased with the amount of perovskite, although this efficiency could be restored by adding carbon to the reactor. Experiments using optical emission spectroscopy (OES) and in situ X-ray photoemission spectroscopy (XPS) were carried out to gain insight into the synergetic effects found with the catalyst. OES intermediate species, including NH*, CN*, CO*, and CH*, were found in the plasma. XPS experiments of samples exposed to plasmas showed the formation of –NO_x and –CN species, indicating the active involvement of the catalyst in the reaction.

Keywords: Plasma catalysis; Plasma chemistry; Perovskite catalyst; In situ XPS; Optical emission spectroscopy; CO oxidation; CH_4 oxidation; NO removal; Soot particles

1. Introduction

Removal of CO, CH_x, NO, SO_x, and other compounds from exhaust combustion sources is a major challenge for environmental protection [1–3]. The most typical procedures used to remove these noxious gases are based on catalysts that can induce different selective oxidation/reduction processes [1–3]. Another possibility that has begun to be explored recently is the combination of catalysts and plasmas to induce specific reactions under mild thermal conditions. Cold plasmas have typically been studied by researchers interested in the characterization of the plasma parameters (e.g., electron temperature, concentration of different active species) [4–9] and by materials scientists for treating or preparing new materials [10–13] or even catalysts [14]. In contrast, the plasma chemistry of complex gas mixtures, alone or in the presence of catalysts, is not a well-developed subject, and much work is needed to improve the performance of these processes for practical applications [15]. Plasma catalytic processes are used mainly in various decontamination processes in which the concentration of pollutants is in the ppm range, including the abatement of volatile organic compounds [16–19], oxidation of light hydrocarbons [20,21], oxidation of CO [16,20], combustion of soot particles [22,23], and removal of NO_x or N_2O from simulated exhaust gases [15,24–33]. Nonetheless, relatively few works have focused on the simultaneous removal of these noxious gases in complex mixtures [15,25,34].

Most designs that use a mixed plasma + catalyst approach are merely the online connection of two independent processes; first, the plasma stage produces a certain reaction, and then the catalyst stage transforms these primary products into secondary final products [17,31,35]. Less frequently, plasma and catalysts are combined together in such a way that the catalyst is em-

* Corresponding author.
E-mail address: arge@icmse.csic.es (A.R. González-Elipe).

0021-9517/$ – see front matter
doi:10.1016/j.jcat.2007.02.006

bedded in a plasma phase rich in radicals and other activated species [16,17]. In this latter case, despite the observation of synergetic effects, it is not clear yet whether the role of the catalyst is just to favor the combination on its surface of the active species of the plasma, or if it participates actively in the reaction. In general, in these plasma hybrid systems, the catalyst activity is typically correlated with its surface area and porosity, regardless of their chemical formulation [15,16,20].

The present work deals with the plasma catalytic removal of NO and the oxidation of CH_4 from complex mixtures consisting of NO, CH_4, and O_2 as minority components and Ar or N_2 as carrier gases. Previous plasma investigations in our laboratory with a microwave (MW) surfatron device in the absence of catalysts have revealed that for such mixtures, the NO is efficiently converted into N_2 and O_2 [36]. Simultaneously, CH_4 is oxidized to CO, a noxious gas that should be removed for practical decontamination applications.

In the present investigation, we used a mixed plasma + catalyst system in an attempt to achieve the oxidation of CO into CO_2. Our results support the utility of this experimental approach and demonstrate the synergetic effects of CO plasma + catalyst oxidation at low temperatures. We used two types of catalysts, a commercial high-specific surface area SiO_2 catalyst and a perovskite-type catalyst prepared in our laboratory. The latter choice was dictated by the fact that perovskite catalysts are well-known catalysts for CO and CH_4 oxidation reactions [37,38]. We used the SiO_2 for comparative purposes to evaluate the hypothesis proposed in several papers in the sense that only the porosity of the catalyst is controlling the efficiency of the plasma + catalyst systems [16,20]. The main focus of the present investigation with complex gas mixtures containing NO, CH_4, and O_2 is to understand the chemical and plasma processes involved in the removal of NO and the conversion of CO (a primary product of the plasma reaction) into CO_2 when the plasma is used in conjunction with a perovskite catalyst. In addition, the beneficial effect of the presence of carbon together with the catalyst for the NO removal was also addressed in the context of this investigation. This carbon simulates the soot particles eventually present in most combustion outlets [15,25,37].

2. Experimental

2.1. Catalyst preparation and characterization

The two catalysts used for the present investigation are a commercial SiO_2 powder from Aldrich with a specific surface area of 270 $m^2\,g^{-1}$ and a $La_{0.5}Sr_{0.5}CoO_{3-d}$ perovskite prepared by spray pyrolysis [39] in our laboratory, with a specific surface area of 13 $m^2\,g^{-1}$. In addition, in some experiments, the perovskite was thoroughly ground with carbon nanoparticulates at a ratio of 90:10 by weight. The carbon, provided by Cabot, had a specific surface area of 190 $m^2\,g^{-1}$.

Perovskite preparation involved the uniform nebulization of nitrate solutions containing $La(NO_3)_3{\cdot}6H_2O$ (99.99%, Aldrich), $Co(NO_3)_2{\cdot}6H_2O$ (>98%, Fluka), and $Sr(NO_3)_2$ (>99%, Fluka) prepared as a 0.1 M liquid solution of precursors. Two online furnaces at 250 and 600 °C evaporated the solvent (distilled water) with the dissolved nitrates and produced an initially amorphous perovskite powder. The material was collected by a porous frit of quartz located in the outlet of the heating system. Subsequently, the powders were annealed at 600 °C for 4 h, thus obtaining a crystalline perovskite with rhombohedral symmetry [40], as evidenced by the X-ray diffractograms shown in Fig. 1a. The ultrasonic nebulization method of liquid droplets favors the formation of pseudospherical particles with a wide range of sizes, as inferred from the scanning electron microscopy (SEM) image shown in Fig. 1b. The mean diameter of particles varied from 200–500 nm to 1 μm, although smaller nanocrystalline domains of 50–60 nm were calculated by applying Scherrer's equation to the main diffraction peaks of this sample.

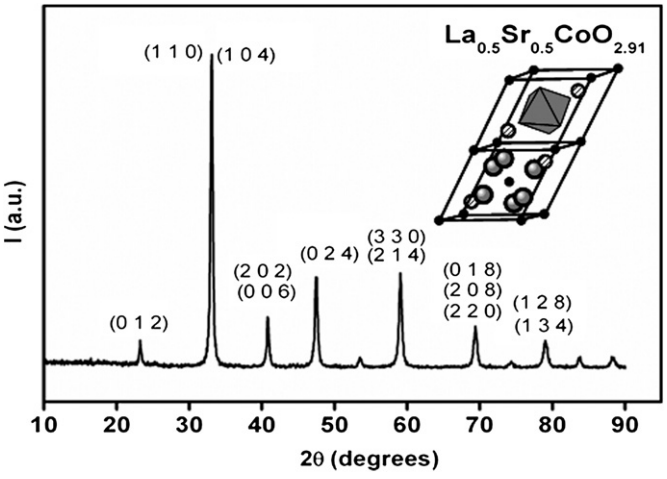

(a)

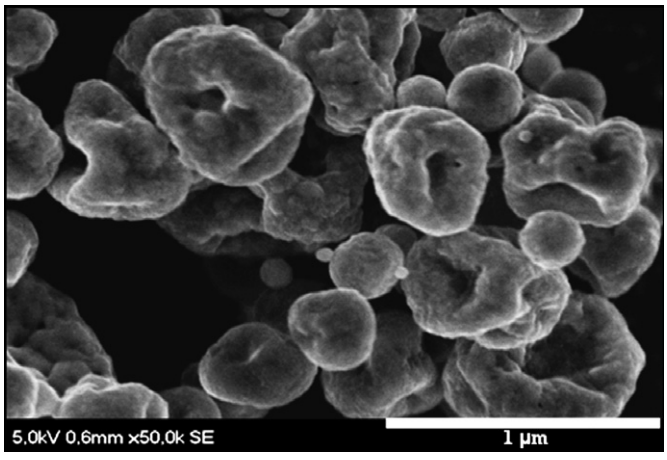

(b)

Fig. 1. (a) XRD pattern of the $La_{0.5}Sr_{0.5}CoO_{3-d}$ perovskite and scheme of the rhombohedral distorted geometry. (b) SEM micrograph of the perovskite catalyst.

2.2. Catalytic activity in the absence of plasma

Catalytic oxidation experiments of CO and CH_4 were carried out at atmospheric pressure in a fixed-bed stainless steel U-shaped reactor; 100 mg of perovskite particles were sustained between quartz wool in approximately the middle of the

reactor. The temperature was controlled by a chromel–alumel thermocouple placed at the catalyst position. The reactor was placed vertically in the center of an electric furnace electronically controlled and provided with another thermocouple.

Before catalytic testing, the catalysts were preoxidized in a stream of synthetic air (>99% purity) at 650 °C for 2 h. This treatment ensured that the perovskite had the same oxidation state in all experiments. The reaction mixtures were fed through UNIT mass flow controllers with a total flow of 100 ml min^{-1} and He as gas balance. The concentrations of the reactants were 0.5% CH_4–5% O_2 and 2% CO–5% O_2 in volume, respectively. The heating rate was 1 °C/min up to maximum temperatures of 500 °C for CO oxidation and 650 °C for methane oxidation. A gas chromatograph provided with a Porapak packed column and a thermal conductivity detector was connected online to analyze the reaction products.

2.3. Plasma characterization

The activated species present in the glow discharge of the plasma were characterized by optical emission spectroscopy (OES), a very powerful, nonintrusive diagnostic tool for detecting in situ reactive plasma species and providing information about the populations of atomic and molecular species in excited states [5,13,41,42]. The experimental setup consisted of an optical fiber to collect the light coming from the plasma glow, connected to a Jobin Ybon (HR250) scanning monochromator and a Hamamatsu photomultiplier tube R928. The emitted spectra are then collected and plotted by a computer. This analysis was done by placing the optical fiber in the position indicated in Fig. 2. The maximum resolution of the spectra was 0.05 nm, and the estimated energy density [43] was ca. 10 W cm^{-3}.

2.4. Plasma catalytic hybrid system

The plasma experiments were carried out in a plasma reactor consisting of a quartz tube (3.5 mm i.d.) similar to that described previously [36,44,45] in studies of the plasma reactivity of complex gas mixtures containing NO, CH_4, and O_2 in the presence of Ar [36] or N_2 [45] as a carrier gas. The plasma was ignited with a surfatron [46] device connected to a MW power supply. A MW power of 75 W was used in all experiments, and the pressure of the gases was maintained at 4 Torr. (This low pressure is necessary to keep the plasma excited.) Details of gas sample dosing, plasma excitation, and detection of reactants/products (the latter by mass spectrometry) have been provided previously [36,44,45]. In the present work, N_2 or Ar was used as a carrier gas, with 3600 ppm of CH_4, 3000 ppm of NO, and 3×10^4 ppm of O_2 added as minor components. Experiments were done with both ternary (O_2, CH_4 plus the carrier gas) and quaternary (O_2, CH_4, NO plus the carrier gas) mixtures.

A scheme of the reactor, composed entirely of quartz, is shown in Fig. 2. The reactor used here was a modified version of that used in previous investigations. The new configuration provides a way to incorporate the catalysts downstream the plasma reaction zone. The reactor zone with the catalyst has a 1-inch o.d. The powder was placed just below the plasma excitation region, still inside the glow zone of the plasma discharge, 10 cm from the surfatron (see Fig. 2). This configuration allows the active species coming from the plasma to interact directly with the catalyst surface. The catalyst zone can be heated by an external furnace to check the effect of temperature on reaction efficiency. The temperature was controlled by a thermocouple placed at the external wall of the reactor near the catalyst region. The amount of catalyst (perovskite or SiO_2) was adjusted to 100 mg, similar to the experiments with the conventional catalytic reactors.

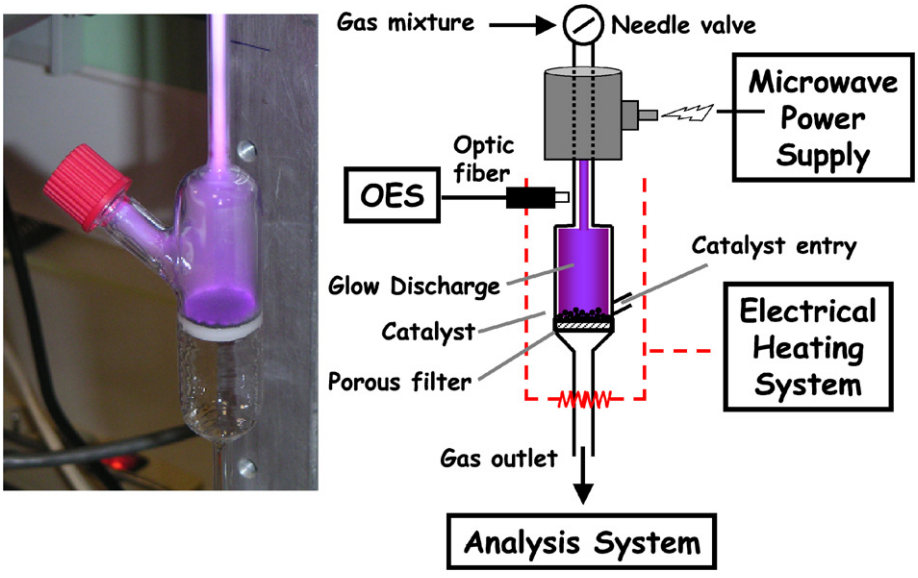

Fig. 2. Schematic view of the plasma + catalyst reactor used for the experiments. The different parts of the system are indicated in the figure. Detail of the plasma reactor. (For color figure the reader is referred to the web version of this article.)

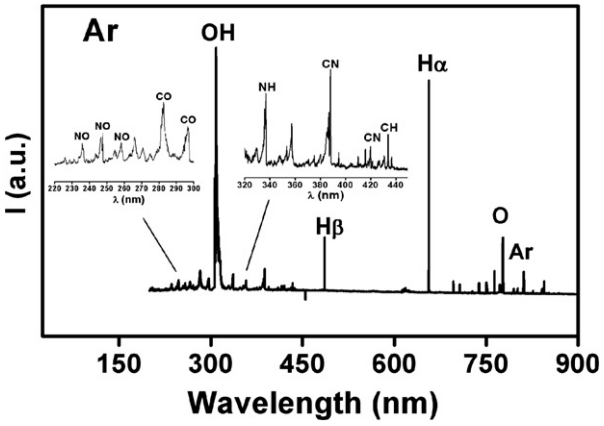

(a)

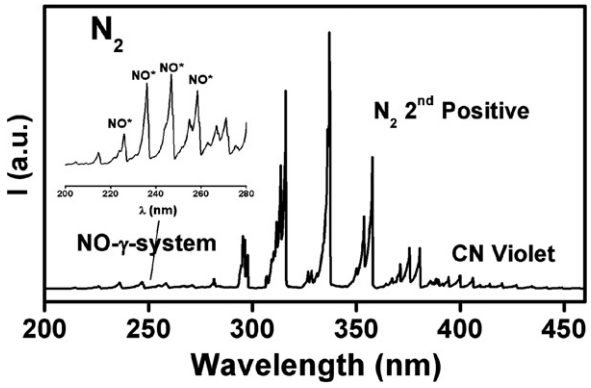

(b)

Fig. 3. OES spectra of the Ar + O_2 + CH_4 + NO (a) and N_2 + O_2 + CH_4 + NO (b) plasmas during reaction conditions. The insets show in an enlarged scale some zones of the spectra to clearly distinguish bands attributed to different species.

2.5. X-ray photoemission spectroscopy characterization

X-ray photoemission spectroscopy (XPS) experiments were carried out on a VG ESCALAB 210 apparatus provided with a prechamber in which in situ plasma experiments can be carried out. For this purpose, a plasma source was inserted in the prechamber, in which catalyst or solid samples can be exposed directly to the plasmas of different gas mixtures. More details on this system were given in a recent study on the interaction of different plasmas with the surface of carbon [47]. The spectra were excited with the Mg$K\alpha$ radiation of the X-ray source and were calibrated in energy by referencing the binding energy (BE) scale of the spectra to the C 1s peak of the adventitious carbon present on the surface of the catalyst. Experiments were carried out after exposing the perovskite catalyst or mixtures of catalyst + carbon to Ar + NO or N_2 + NO plasmas (3000 ppm NO in the gas mixture) for increasing periods. The pressure was maintained at 0.04 Torr during these plasma treatments.

3. Results

3.1. OES analysis of plasma

A difference between conventional catalytic- and plasma-activated reactions is that in the latter, radicals, ions, and other activated neutral species exist in the plasma and may react in the gas phase. In addition, an equivalent concentration of free electrons, usually bearing a high kinetic energy, is also present to compensate for the positive charge of the ionized species [48]. For the gas mixtures investigated in the present work, Fig. 3a provides an indication of the type of intermediate species formed in the gas phase that account for the overall reactivity of the system in the absence of catalyst. This figure reports OES spectra of the plasma formed with the quaternary gas mixture and Ar as carrier gas. A thorough analysis of this type of spectra has been published recently [36,45]. For the purposes of the present investigation, it is worth stating that peaks and bands attributed to CO*, OH*, CH*, H*, and O* species are clearly distinguished in the spectra [42]. These and other similar species not yielding emission lines must be responsible for the reactivity of the plasma when using Ar as a carrier gas. With N_2 used as a carrier gas, the spectrum in Fig. 3b is dominated by bands due to N_2^* species (second positive system) [42], with small contributions of CN* and NO* species and other species (e.g., N_2^+, NH*) not easily detectable at the scale used for the representation. The plasma reaction likely involving these species produces the complete removal of NO, converted into N_2 and O_2, and the combustion of CH_4, converted mainly into CO and H_2O. We have discussed the mechanisms involved in the corresponding plasma reactions in previous works [36,45].

Table 1
Summary of CH_4 and NO removal efficiencies and selectivity of CO_2 formation by plasma reactions of ternary and quaternary gas mixtures

Gas mixtures	Treatments[a]	% CH_4 decomposition yield	% NO decomposition yield		% CO_2 selectivity	
			Ar[b]	N_2[b]	Ar	N_2
CH_4:O_2	MWD[c]	95–99	–	–	10	8
CH_4:O_2:NO	MWD	97–99	88	68	8	6

[a] All treatments are referred to room temperature.
[b] Carrier gas.
[c] Microwave flowing discharge.

3.2. Plasma catalysis for CH_4 oxidation in ternary mixtures: Effect of temperature

For a practical application of the plasma technology data given in Table 1, the main results of the plasma reactions indicate highly efficient NO removal but with high amounts of CO production. In an attempt to define an integrated process in which both NO and CH_4 can be removed without producing high amounts of CO, we consider the possibility of using the plasma in conjunction with a catalyst. Using the reactor described in Fig. 2, we first studied the efficiency of the process for ternary gas mixtures in the absence of NO. Table 1 shows that plasma excitation of this ternary mixture without catalyst produced the almost complete removal of CH_4, which was converted into CO + H_2O. In this process, only about 10% of the initial CH_4 was converted into CO_2 (cf. Table 1). In the presence of a catalyst, the amount of CH_4 transformed into CO_2 increased up to approximately 40% with both the perovskite

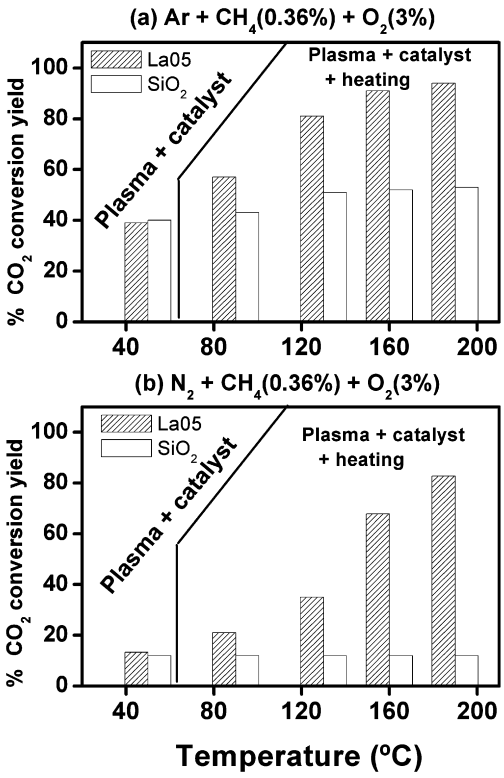

Fig. 4. Percentage of CH_4 converted into CO_2 as a function of temperature in the plasma hybrid system in the presence of SiO_2 and $La_{0.5}Sr_{0.5}CoO_{3-d}$. (a) Ternary mixture with Ar as carrier gas. (b) Ternary mixture with N_2 as carrier gas.

and the SiO_2 catalysts (Fig. 4). It is very interesting that the conversion efficiency was temperature-dependent and reached a value of about 90% at 190 °C in experiments using either Ar or N_2 as a carrier gas. It is also noteworthy that when SiO_2 was used as the catalyst, temperature had no significant effect on the conversion yield, although differences did occur depending on whether Ar (conversions of 40–45%) or N_2 (conversions of ca. 10%) was used as a carrier gas.

In connection with these plasma + catalyst results, it is interesting to consider the catalytic activity of the perovskite catalyst for conventional oxidation reactions. Fig. 5 reports the oxidation yields of CO and CH_4 into CO_2. CO oxidation started at ca. 250 °C and was almost complete at 350 °C. Methane oxidation required much higher temperatures than CO oxidation, with an onset temperature of about 500 °C. Although the oxidation rate increased with temperature, only 65% methane was converted into CO_2 at 650 °C under our experimental conditions. These results are in line with those of other similar catalytic processes reported in the literature [38] and clearly support the notion that plasma activation of the perovskite catalysts constitutes a singular process that enables the almost complete conversion of CH_4 into CO_2 at 200 °C.

3.3. Plasma catalysis in quaternary mixtures: Effect of adding NO

The aim of this investigation was to define an integrated system in which both NO and CH_4 can be removed without any significant production of CO. Along these lines, experiments were carried out with the quaternary mixture (i.e., CH_4, O_2, and NO with either Ar or N_2 as a carrier gas) to determine whether the presence of catalyst affects the overall performance of the system. Fig. 6 compares, in the form of a bar diagram, the efficiency of NO removal in three different experiments: (i) plasma discharge without catalyst, (ii) plasma discharge in the presence of catalyst, and (iii) plasma discharge in the presence of perovskite catalyst mixed with graphitic carbon. This latter situation simulates the effect of the soot particles that usually accompany the exhaust gases by the NO/CH_x removal processes. This figure clearly shows that the catalyst produced a drastic decrease in NO removal, particularly when N_2 was used as carrier gas. In comparison, the catalyst + carbon mixture partially restored the efficiency of the process. The effects of the interaction of the plasma on the surface of the catalyst were further

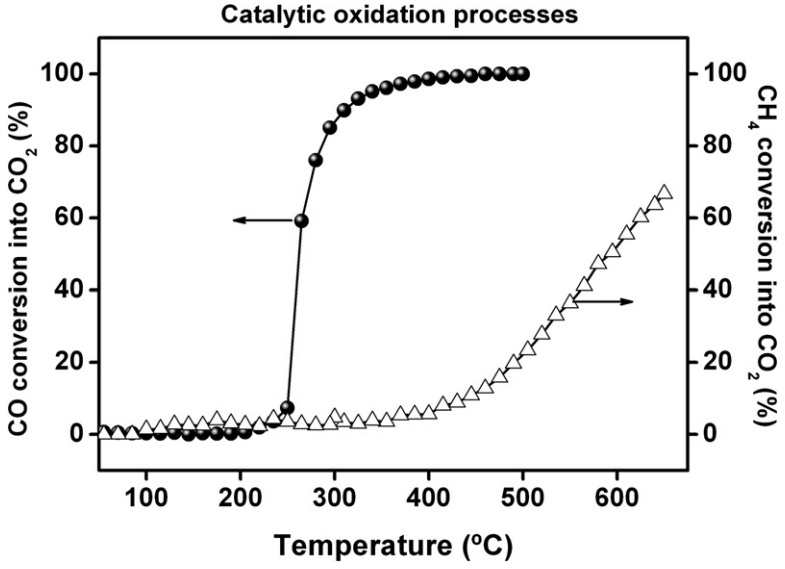

Fig. 5. Percentage of CO and CH_4 converted into CO_2 as a function of temperature for conventional catalytic oxidation processes.

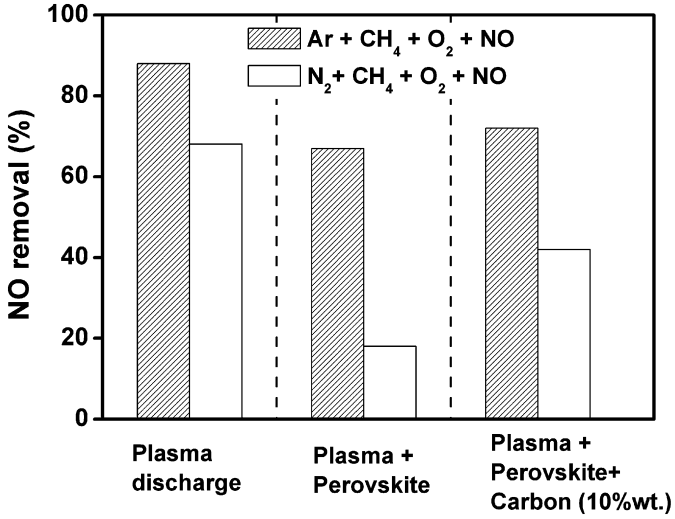

Fig. 6. NO conversion efficiencies at room temperature for quaternary mixtures with either Ar or N_2 as carrier gas and three different experimental situations: plasma process, plasma in the presence of the perovskite catalysts and plasma in the presence of a mixture of the perovskite catalyst plus carbon.

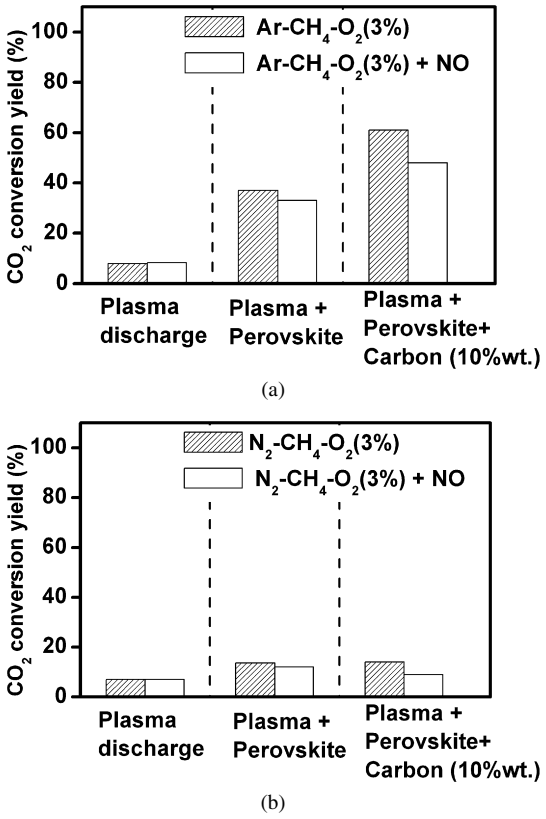

Fig. 7. Effect of the NO addition on the CH_4 into CO_2 conversion yield at room temperature with either Ar (a) or N_2 (b) as carrier gas and three different experimental situations: plasma process, plasma in the presence of the perovskite catalysts and plasma in the presence of a mixture of the perovskite catalyst plus carbon.

investigated by XPS; the results are described below and discussed in more detail in Sections 4.2 and 4.3.

Another point that must be considered when evaluating the possible practical applications of this type of plasma + catalyst process is the influence on the conversion yield of CH_4 into CO_2 when NO is added to the reaction mixture. Fig. 7 compares, in the form of bar diagrams, the CO_2 conversion efficiencies for ternary and quaternary mixtures. For the three investigated situations, these diagrams show that, compared with the ternary mixture results, the conversion efficiency of CH_4 into CO_2 was only slightly lower in the presence of NO.

3.4. XPS investigation of plasma–catalyst interactions

The previous results demonstrate that the incorporation of a catalyst into the plasma discharge may alter the distribution of products. In particular, Fig. 6 shows that the efficiency of NO removal is drastically reduced by the presence of the perovskite catalyst when compared with plasma-alone experiments. To identify the reasons for this decrease and its partial recovery when the catalyst is mixed with carbon, we carried out a series of XPS experiments in which the catalyst or catalyst + carbon mixtures were exposed in situ to plasmas of Ar(N_2) + NO. These experiments have provided information about the intermediate species formed on the surface of the perovskite exposed to these plasma discharges containing NO.

Fig. 8 shows a series of N 1s photoemission peaks taken from the perovskite surface exposed to these plasmas for increasing periods. The spectrum of the original sample has some small peaks with BEs of 406–407.5 eV that can be attributed to $–NO_2$ and $–NO_x$ ($x \leqslant 2$) adsorbed species [47,49,50]. However, the most remarkable features of this experiment are the changes observed in the intensity of the N 1s peaks as a function of the exposure time to the plasmas. For the two plasma mixtures, a common observation is a sharp increase in the intensity of these N 1s peaks after exposure times of 20 min in Ar and 10 min in N_2 and a subsequent decrease in both cases at longer exposure times. In addition, a small peak at around 398 eV attributed to adsorbed –CN species also can be observed for long exposure times [47,51]. Besides the N 1s peak, the other elements present in the sample were also investigated by this photoemission experiment; however, the Co 2p, La 3d, O 1s, or Sr 3d spectra demonstrated no significant variation in shape and/or intensity after these plasma exposure experiments and are not reported here.

The results of a similar experiment carried out with a catalyst + carbon mixture are presented in Fig. 9. In this case, the peak at 407.5 eV, attributed to $–NO_2$ species, remained in the spectra even after longer exposure times to the two plasmas. In addition, the peak at around 398 eV attributed to –CN species progressively increased in intensity with exposure time. According to previous experiments in which pure carbon was exposed to similar plasma mixtures [47], formation of –CN species occurs on the surface of carbon exposed to this type of plasma and here must be considered a consequence of the presence of carbon in the treated samples. Meanwhile, the two other species appearing at 406 and 407.5 eV can be formed on both the perovskite and the carbon surfaces, in the latter case remaining with high intensity after long exposure times (cf. Figs. 8 and 9). It is also worth mentioning that, as shown in Fig. 10, plasma treatment of the perovskite + carbon mixtures produced a significant (20%) decrease in intensity of the C 1s peak at 284.6 eV, attributed to

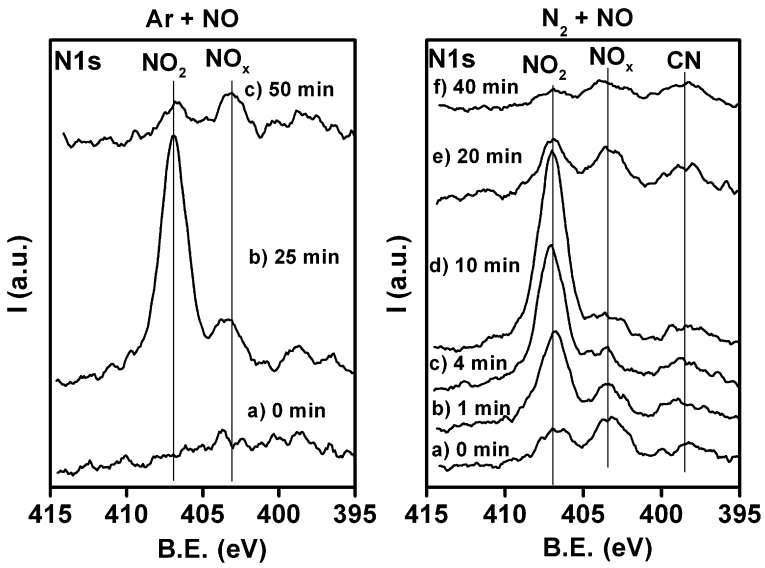

Fig. 8. N 1s photoemission spectra of the perovskite exposed for increasing periods of time to a plasma of Ar + NO (left) or N_2 + NO (right).

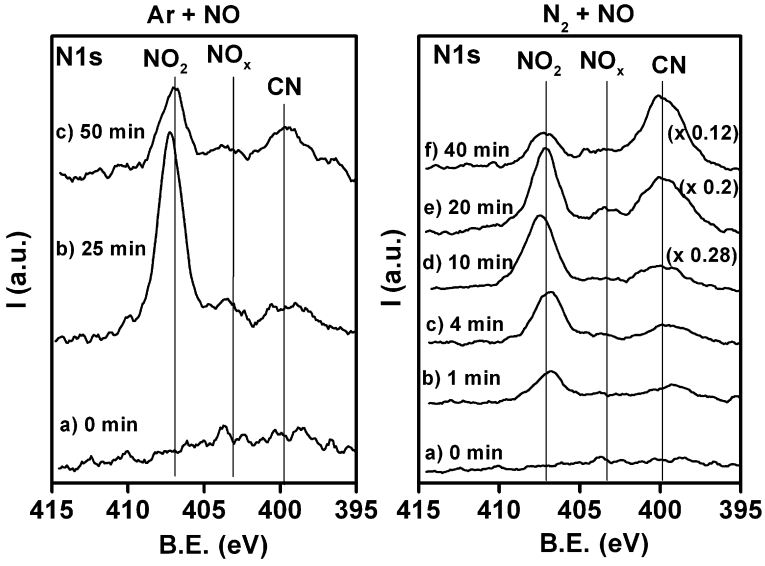

Fig. 9. N 1s photoemission spectra of the mixture perovskite + carbon exposed for increasing periods of time to a plasma of Ar + NO (left) or N_2 + NO (right). Scale factor corrections are included in some spectra.

graphitic or aliphatic carbon. The spectra in this figure present two components, one at 284.6 eV and another at ca. 289 eV, due to COO^- and related species formed on the surface of carbon or to $-CO_3^-$ species formed on the surface of the perovskite.

4. Discussion

In what follows we will treat partial aspects of the work carried out here separately and conclude with an overall assessment of the possibilities of plasma + catalyst processes in the removal of noxious components from exhaust gases.

4.1. Synergy by the oxidation of CH_4 (CO) with plasma + catalyst systems

For ternary mixtures, the results summarized in Fig. 4 clearly demonstrate that the plasma + catalyst system is very effective for inducing the oxidation of CH_4 into CO_2. This result contrasts with those summarized in Table 1 corresponding to similar reactions without catalyst. The data in this table indicate that methane is converted almost totally into CO and H_2O (only 10% CO_2 conversion) in plasma-only conditions. Thus, it is evident that incorporating the catalysts into the process favors the posterior oxidation of CO into CO_2. According to Fig. 4, the efficiency of the oxidation to CO_2 depends on the type of catalyst and the type of carrier gas in the gas mixture. The data in this figure indicate that the oxidation efficiency to CO_2 was relatively higher with Ar as a carrier gas than with N_2 as a carrier gas, particularly when working at low temperature (i.e., 40–50 °C) due to the effect of the plasma. Another significant difference in these plasma + catalyst processes is that at 40 °C, the SiO_2 rendered conversion efficiencies of CH_4 into CO_2 on the order of 40% with Ar but only 10% with N_2.

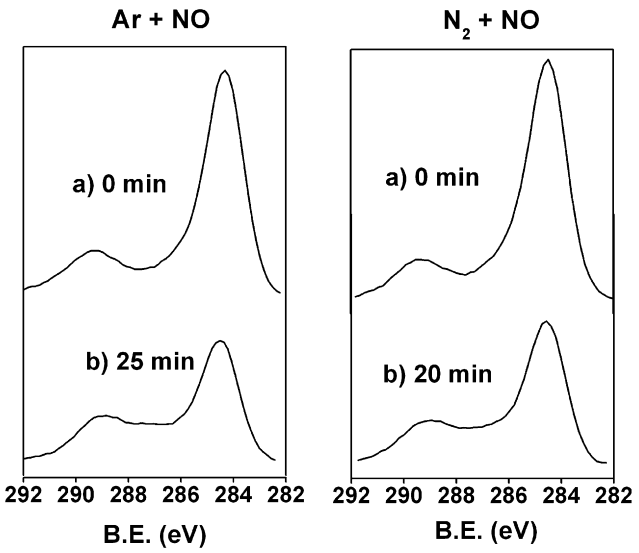

Fig. 10. C 1s photoemission spectra of the mixture perovskite + carbon exposed for increasing periods of time to a plasma of Ar + NO (left) or N_2 + NO (right).

The enhanced CO oxidation efficiency when using Ar as a carrier gas can be accounted for by considering the intermediate species detected in the plasma. The intensity of the OES bands due to CO*, OH*, and O* is much higher with Ar than with N_2. It is also common knowledge in plasma physics that for equivalent working conditions, Ar plasmas present higher electron temperatures and densities than nitrogen plasmas [52,53]. This is due to the existence of a wider diversity of channels for the depletion of electrons in the case of molecular species such as nitrogen (i.e., vibrational and rotational excitation, dissociative ionization) than in Ar (i.e., mainly metastable states) [53]. Thus, the high reactivity found at low temperatures with Ar as carrier gas likely results from direct reactions on the surface of the catalysts of CO (CO*) and O* (OH*) species. The lower concentrations of these species (and electrons) in the plasma of the ternary mixture with N_2 should be the reason for the lower CH_4 oxidation efficiency found for this gas mixture.

The results in Fig. 4 also show that the conversion yield into CO_2 increased with temperature when perovskite was used as a catalyst. A similar enhancement was not found with SiO_2. This increased perovskite reactivity with temperature indicates that some surface activation was induced by both the plasma and the effect of heating up to 200 °C. In this sense, it is interesting to note that no oxidation of either CO or CH_4 was detected at $T \leqslant 200$ °C by conventional thermal processes (cf. Fig. 5). Although additional information is needed, we believe that the plasma + catalyst synergetic effects demonstrated in Fig. 4 are related to the formation of new active species of oxygen onto the surface of the perovskites when they are exposed to activated species of oxygen like the O* or OH* detected by OES (cf. Fig. 3).

Another common effect of the interaction of plasmas with solids is the etching of their surfaces [13,14]. Cleaning or removing certain species from the surfaces of the perovskites by interaction with the plasma would provide adsorption sites for the CO molecules (or CO* species), a process known to be a limiting step by the thermal oxidation of CO [54].

In summary, our plasma + catalyst experiment shows that the oxidation of methane occurs through novel mechanisms that imply not only the direct interaction on the catalyst surface of CO (CO*) species and activated species of oxygen, but also the opening on the perovskite surface of new reaction routes between them induced by both the plasma interaction and the heating of the solid.

4.2. Decrease in the capacity of NO removal in the presence of the catalyst

We have found that the incorporation of the perovskite catalyst produces a sharp decrease in the efficiency of NO removal (cf. Fig. 6). In this way, the beneficial effect of the catalyst in the oxidation of CO is detrimental with respect to the NO removal capacity. The decreased removal efficiency must be a result of recombination processes between plasma species occurring on the catalyst surface. Results of the XPS experiments in which the perovskite was exposed to Ar(N_2) + NO plasmas provide some clues as to the nature of these recombination processes. Figs. 8 and 9 show that –NO_x and –NO_2 adsorbed species were formed onto the surface of the perovskite exposed to these plasmas. The concentration of these species passed through a maximum and decreased when steady-state conditions are reached. The OES spectra in Fig. 3 shows that a high concentration of NO* species were formed in the plasma of quaternary mixtures. A similar situation was found for Ar(N_2)–NO mixtures [36,45]. These excited NO* species can be very reactive toward any oxide surface. In the gas phase, these intermediate species readily dissociate into N_2 and O_2 as final products [36,45]. However, in the presence of the perovskite, these species and eventually others containing nitrogen (e.g., N_2^+) likely will interact with the oxide ions of the catalyst surface and give rise to the –NO_x and –NO_2 adsorbed species [55] detected by XPS (cf. Figs. 8 and 9). Decomposition of these species as an effect of the surface bombardment by the other plasma species and/or free electrons in the plasma yields NO and thus contributes to the decreased removal efficiency of the system toward this minority component.

4.3. Effect of carbon on the removal of NO

Figs. 6 and 7 demonstrated that incorporating carbon into the process restored its capacity to remove NO without affecting the oxidation efficiency of CO/CH_4 into CO_2. Soot is a usual component of the exhaust gases from many combustion processes [22,23,37], and this it should have a similar role as the carbon used in our experiment. The beneficial effect of carbon can be explained with the help of the results of the XPS experiment shown in Fig. 9. According to these photoemission spectra, besides the development of –NO_x and –NO_2 species, likely formed mainly on the surface of the perovskite, the interaction of the catalyst + carbon mixture with the Ar(N_2) + NO plasmas induced the formation of –CN species. According to previous XPS investigations on carbon [51], such species are intermediates of the reduction of NO by carbon according to a process like NO + C → –CN(ads) → N_2. The detection

of these –CN adsorbed species by XPS supports the supposition that the activity of carbon toward $Ar(N_2) + NO$ plasmas is not affected by the presence of the catalyst. The fact that carbon can be considered another reactant of the process is further confirmed by the results in Fig. 10 showing that the intensity of the C 1s peak attributed to graphitic or aliphatic carbon decreased with the exposure time to the $Ar(N_2) + NO$ plasma.

5. Conclusion

Plasma-catalytic processes are attracting the attention of many researchers interested in developing new methods of treating exhaust gases [15,16,19,20,25,27,29]. At the present stage, most of the works in this field rely on an empirical approach in which the efficiency is empirically correlated with the different parameters of the process. In the present work, we aimed to develop an integrated experimental methodology that takes into account both the plasma parameters and the process efficiency. We used spectroscopic analysis of the plasma by OES and that of the surface of the catalyst by XPS to evaluate the active species of the plasma intervening in the reactions and the intermediate species formed on the surface of the catalyst exposed to the plasma. Combining all of this information with the results of CH_4 oxidation and NO removal, we were able to demonstrate that the role of the perovskite catalyst in the process is not limited to providing surface reaction sites at which active plasma species can react among them. This effect, which has been claimed for other plasma + catalyst processes [15,16,20] and observed here for SiO_2, is complemented in the case of the perovskite with its direct participation in the oxidation of CO into CO_2 at temperatures of up to 200 °C.

We also found that the presence of the perovskite is detrimental to the efficiency of NO removal. The interaction of the active NO^* and other nitrogen plasma species with the surface of the perovskite provides a route for the formation of new NO molecules that compensate for those dissociated in the plasma. A possible approach to overcoming this problem is to add carbon to the catalyst. This carbon acts as another reactant of the process and, by reacting directly with the NO^* species, leads to its reduction into N_2. In this way, the presence of soot particles in the exhausts of most combustion processes should not be considered a negative factor, but rather a source of an efficient reducing agent that, when activated with the plasma, favors the decomposition of NO into N_2.

Acknowledgments

Financial support was provided by the Ministry of Science and Education of Spain (projects PPQ2001-3108 and ENE2004-01660 and a doctoral fellowship for J.L.H.). We thank Cabot for providing the carbon nanoparticulates. We also appreciate the collaboration of Dr. J.P. Holgado with the SEM images and Dr. Ocaña for his helpful assistance in the development of the spray pyrolysis experimental setup.

References

[1] J.N. Armor, Catal. Today 38 (1997) 163.
[2] J.N. Armor, Appl. Catal. B Environ. 1 (1992) 221.
[3] F. Garin, Catal. Today 89 (2004) 255.
[4] R. Atkinson, D.L. Baulch, R.A. Cox, R.F. Hampson, J.A. Kerr, J. Troe, J. Phys. Chem. Ref. Data 18 (1989) 881.
[5] E.A.H. Timmermans, J. Jonkers, A. Rodero, M.C. Quintero, A. Sola, A. Gamero, D.C. Schram, J.A.M. van der Mullen, Spectrochim. Acta Part B At. Spectrosc. 54 (1999) 1085.
[6] A. Ricard, C. Jaoul, F. Gaboriau, N. Gherardi, S. Villeger, Surf. Coat. Technol. 188–189 (2004) 287.
[7] J.T. Herron, D.S. Green, Plasma Chem. Plasma Process. 21 (2001) 459.
[8] D.L. Baulch, C.J. Cobos, R.A. Cox, C. Esser, P. Frank, T. Just, J.A. Kerr, M.J. Pilling, J. Troe, R.W. Walker, J. Warnatz, J. Phys. Chem. Ref. Data 21 (1992) 411.
[9] V. Guerra, P.A. Sa, J. Loureiro, J. Phys. D Appl. Phys. 34 (2001) 1745.
[10] A. Borrás, A. Barranco, A.R. González-Elipe, J. Mater. Sci. 41 (2006) 5220.
[11] F. Gracia, F. Yubero, J.P. Holgado, J.P. Espinós, A.R. González-Elipe, T. Girardeau, Thin Solid Films 500 (2006) 19.
[12] A. Martín, J.P. Espinós, A. Justo, J.P. Holgado, F. Yubero, A.R. González-Elipe, Surf. Coat. Technol. 151 (2002) 289.
[13] A. Barranco, J. Cotrino, F. Yubero, J.P. Espinós, J. Benítez, C. Clerc, A.R. González-Elipe, Thin Solid Films 401 (2001) 150.
[14] M.B. Kizling, S.G. Jaras, Appl. Catal. A Gen. 147 (1996) 1.
[15] B.S. Rajanikanth, A.D. Srinivasan, V. Ravi, IEEE Trans. Dielect. Elect. Insul. 12 (2005) 72.
[16] F. Holzer, U. Roland, F.D. Kopinke, Appl. Catal. B Environ. 38 (2002) 163.
[17] H.H. Kim, Plasma Process. Polym. 1 (2004) 91.
[18] C. Subrahmanyam, A. Magureanu, A. Renken, L. Kiwi-Minsker, Appl. Catal. B Environ. 65 (2006) 150.
[19] M. Magureanu, N.B. Mandache, P. Eloy, E.M. Gaigneaux, V.I. Parvulescu, Appl. Catal. B Environ. 61 (2005) 12.
[20] A. Rousseau, A.V. Meshchanov, J. Roepcke, Appl. Phys. Lett. 88 (2006).
[21] M. Heintze, B. Pietruszka, Catal. Today 89 (2004) 21.
[22] A.R. Martin, J.T. Shawcross, J.C. Whitehead, J. Adv. Oxid. Technol. 8 (2005) 126.
[23] J. Grundmann, S. Muller, R.J. Zahn, Plasma Chem. Plasma Process. 25 (2005) 455.
[24] S. Broer, T. Hammer, Appl. Catal. B Environ. 28 (2000) 101.
[25] J.O. Chae, J.W. Hwang, J.Y. Jung, J.H. Han, H.J. Hwang, S. Kim, V.I. Demidiouk, Phys. Plasmas 8 (2001) 1403.
[26] K.P. Francke, H. Miessner, R. Rudolph, Catal. Today 59 (2000) 411.
[27] T. Hammer, Plasma Sources Sci. Technol. 11 (2002) A196.
[28] K. Krawczyk, M. Mlotek, Appl. Catal. B Environ. 30 (2001) 233.
[29] H. Miessner, K.P. Francke, R. Rudolph, T. Hammer, Catal. Today 75 (2002) 325.
[30] Y.S. Mok, D.J. Koh, K.T. Kim, I.S. Nam, Ind. Eng. Chem. Res. 42 (2003) 2960.
[31] R.G. Tonkyn, S.E. Barlow, J.W. Hoard, Appl. Catal. B Environ. 40 (2003) 207.
[32] I.S. Yoon, R.G. Tonkyn, A.G. Panov, A.C. Kolwaite, S.E. Barlow, M.L. Balmer, Abstr. Pap. Am. Chem. Soc. 220 (2000) U388.
[33] A.M. Zhu, Q. Sun, J.H. Niu, Y. Xu, Z.M. Song, Plasma Chem. Plasma Process. 25 (2005) 371.
[34] M.X. Pei, H. Lin, W.F. Shangguan, Z. Huang, J. Environ. Sci. 17 (2005) 220.
[35] H. Miessner, K.P. Francke, R. Rudolph, Appl. Catal. B Environ. 36 (2002) 53.
[36] J.L. Hueso, A.R. González-Elipe, J. Cotrino, A. Caballero, J. Phys. Chem. A 109 (2005) 4930.
[37] D. Fino, N. Russo, G. Saracco, V. Specchia, J. Catal. 217 (2003) 367.
[38] M. Alifanti, N. Blangenois, M. Florea, B. Delmon, Appl. Catal. A Gen. 280 (2005) 255.
[39] E. López-Navarrete, A. Caballero, V.M. Orera, F.J. Lázaro, M. Ocaña, Acta Mater. 51 (2003) 2371.
[40] N. Closset, R.v. Doorn, H. Kruidhof, J. Boeijsma, Powder Diffr. 11 (1996).
[41] U. Fantz, Contrib. Plasma Phys. 44 (2004) 508.

[42] R.W.B. Pearse, A.G. Gaydon, in: The Identification of Molecular Spectra, Champan & Hall, New York, 1976.
[43] C.R. Wierenga, T.J. Morin, AIChE J. 35 (1989) 1555.
[44] A. Yanguas-Gil, J.L. Hueso, J. Cotrino, A. Caballero, A.R. González-Elipe, Appl. Phys. Lett. 85 (2004) 4004.
[45] J.L. Hueso, A.R. González-Elipe, J. Cotrino, A. Caballero, J. Phys. Chem. A 111 (2007) 1057.
[46] M. Moisan, Z. Zakrzewski, US Patent 4 906 898 (1990) to Universite de Montreal.
[47] J.L. Hueso, J.P. Espinós, A. Caballero, J. Cotrino, A.R. González-Elipe, Carbon 45 (2007) 89.
[48] B.M. Penetrante, S.E. Schultheis, Non-Thermal Plasma Techniques for Pollution Control, Parts A and B, Springer, Berlin, 1993.
[49] D. Hendricksson, J. Hollande, W.L. Jolly, Inorg. Chem. 8 (1969) 2642.
[50] C.D. Batich, D.S. Donald, J. Am. Chem. Soc. 106 (1984) 2758.
[51] J.R. Pels, F. Kapteijn, J.A. Moulijn, Q. Zhu, K.M. Thomas, Carbon 33 (1995) 1641.
[52] S. Nowak, P. Groning, O.M. Kuttel, M. Collaud, G. Dietler, J. Vac. Sci. Technol. A Vac. Surf. Films 10 (1992) 3419.
[53] E.I. Toader, Plasma Sources Sci. Technol. 13 (2004) 646.
[54] L.G. Tejuca, J.L.G. Fierro, J.M.D. Tascón, Adv. Catal. 36 (1989) 237.
[55] M.A. Peña, J.L.G. Fierro, Chem. Rev. 101 (2001) 1981.